



HAL
open science

On the numerical modeling of compressible forced convection of gases in micro-channels

Chahinez Tchekiken, Eric Chénier, Xavier Nicolas, Guy Lauriat

► **To cite this version:**

Chahinez Tchekiken, Eric Chénier, Xavier Nicolas, Guy Lauriat. On the numerical modeling of compressible forced convection of gases in micro-channels. 5th International Conference on " HEAT TRANSFER and FLUID FLOW in MICROSCALE, Apr 2014, Marseille, France. pp.O-128_146. hal-01006205

HAL Id: hal-01006205

<https://hal.science/hal-01006205v1>

Submitted on 14 Jun 2014

HAL is a multi-disciplinary open access archive for the deposit and dissemination of scientific research documents, whether they are published or not. The documents may come from teaching and research institutions in France or abroad, or from public or private research centers.

L'archive ouverte pluridisciplinaire **HAL**, est destinée au dépôt et à la diffusion de documents scientifiques de niveau recherche, publiés ou non, émanant des établissements d'enseignement et de recherche français ou étrangers, des laboratoires publics ou privés.

On the numerical modeling of compressible forced convection of gases in micro-channels

C. TCHEKIKEN^{1,a}, E. CHENIER^{1,b}, X. NICOLAS^{1,c} and G. LAURIAT^{1,d}

¹Laboratoire MSME, UMR CNRS 8208, Université Paris-Est, 77454 Marne-la-Vallée Cedex 2, France

^achahinez.tchekiken@u-pem.fr, ^beric.chenier@u-pem.fr, ^cxavier.nicolas@u-pem.fr, ^dguy.lauriat@u-pem.fr

Keywords: micro channel, compressible flow, slip flow, thermal jump, thermal creep, viscous dissipation

Abstract. A parametric study of nitrogen flows in a 2D micro channel of 3 μm height and 1.5 mm long, heated at constant flux, is carried out for a wide range of inlet and outlet pressures ($0.9 < p_i < 5$ bars; $0.08 < p_o < 4.9$ bars) corresponding to Knudsen numbers $Kn < 0.1$, Mach numbers $Ma < 1$ and Reynolds numbers $Re < 25$. The numerical model considers the compressibility effects, the viscous dissipation and the rarefaction effects at the wall (velocity slip, temperature jump, thermal creep and viscous work). The domain of validity of simplified models which do not take into account these terms are identified. Correlations between the different quantities characterizing these flows and the parameters Kn , Ma , Re are established.

Introduction

The Navier-Stokes equations can be used to simulate gas flows in micro channels as long as the Knudsen number, Kn , is small enough ($Kn = \lambda/D_h \leq 0.1$, with λ the mean free path of the gas molecules and D_h the hydraulic diameter) and provided that the rarefaction effects at walls (velocity slip, temperature jump and thermal creep) are taken into account when $0.001 < Kn < 0.1$ [1-3]. Furthermore, when $D_h \approx 1$ to 10 μm and the streamwise aspect ratio is large, when the pressure variations between inlet and outlet are around one bar and a few bars, the conversion between the mechanical work of the gas, its internal energy and the viscous heating is important, the Mach and Brinkman numbers can be greater than 1 and the Reynolds and Péclet numbers can vary between 10^{-2} and 10^2 . As a consequence, in addition to the rarefaction effects at the walls, the numerical modeling of this type of flows requires to consider the effects of: (i) compressibility (volume expansion and cooling related to the pressure work) [4-6], (ii) viscous dissipation (heat source) [5, 6], (iii) viscous stress power at the wall in the presence of velocity slip [7, 8], (iv) the variation of the physical properties with temperature [9], (v) the dominant axial diffusion when Re and Pe are smaller than unity, and (vi) the conduction in the walls (conjugate heat transfer) as they are generally thicker and have a higher conductivity than the gas flowing through the duct [10].

A review of the numerous studies on this subject showed that all of these effects are never investigated simultaneously in the mathematical models used. This can be justified in some cases when the effect of the omitted terms is negligible on the dynamic and thermal behavior of the flow. However, the justification for the use of simplifying assumptions in the model is often not provided.

The purpose of this communication is to study all the effects described above (except the conjugate heat transfer) in the case of gas flows in 2D plane micro channels, heated at constant flux, for a wide range of inlet and outlet pressures. The paper focuses on the analysis of the energy equation, temperature field and Nusselt number. A finite volume code is used to solve the full physical model described above or simplified versions of the model. The relative influence of each term of the energy equation and thermal boundary conditions is determined through the computations of the source terms and thermal fluxes at wall. It is shown that the thermal flux balance can be significantly modified by the viscous stress power at the walls and that thermal diffusion at the upstream and downstream sections of the micro channel must be taken into account to appropriately model the thermal creep. In the following, the mathematical model, the numerical method, the analyzed quantities and the results of the parametric study are successively presented.

Mathematical model and numerical method

Geometry. The 2D micro channel used in the present study is displayed in Fig. 1. Its height and length are $H=3 \mu\text{m}$ and $L=1.5 \text{ mm}$. A half channel is simulated due to the symmetry through the horizontal mid plane. The gas used is nitrogen. It enters into the channel at temperature $T_i=300 \text{ K}$. On the wall at $y=H/2$, a heat flux density $q_w=259 \text{ W/m}^2/\text{m}$ is applied. This configuration exactly corresponds to the one used in [6] which has been used as reference to validate the present simulations [11]. A pressure difference $\Delta p=p_i-p_o$ is imposed between inlet and outlet in order to always check that $Kn=\lambda/(2H)\leq 0.1$, $Ma<1$, the inlet pressure $p_i<5 \text{ bars}$ and the maximum temperature $T_{\text{max}}<2000 \text{ K}$. The outlet temperature, T_o , depends on the flow rate and the ratio between the viscous dissipation and the pressure work.

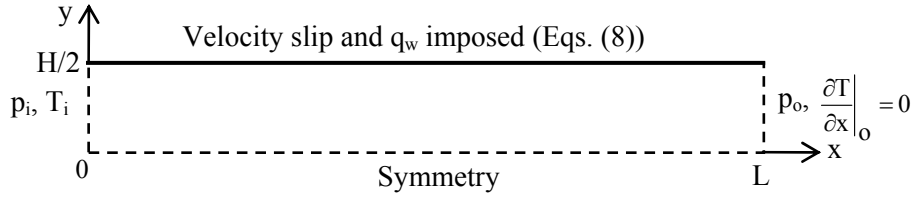


Figure 1 : *Geometry and boundary conditions*

Equations. The steady conservation equations are solved for a Newton-Stokes ideal gas:

$$\nabla \cdot (\rho \vec{v}) = 0 \quad (1)$$

$$\nabla \cdot (\rho \vec{v} \otimes \vec{v}) = -\nabla p + \nabla \cdot \bar{\tau} \quad \text{with} \quad \bar{\tau} = \mu [\nabla \vec{v} + (\nabla \vec{v})^t] - (2/3)\mu \nabla \cdot \vec{v} \bar{I} \quad (2)$$

$$C_p \nabla \cdot (\rho \vec{v} T) - \nabla \cdot (k \nabla T) = \vec{v} \cdot \nabla p + \bar{\tau} : \nabla \vec{v} \quad (3)$$

where $\vec{v} = u\vec{e}_x + v\vec{e}_y$ and the density, conductivity, dynamic viscosity and specific heat capacity of nitrogen vary with temperature according to the following law [6]:

$$\rho = \rho_i(T_i/T)(P/P_i); \quad k = k_i(T/T_i)^{0.77}; \quad \mu = \mu_i(T/T_i)^{0.68}; \quad C_p = C_{p,i}(T/T_i)^{0.078} \quad (4)$$

where the physical properties at inlet temperature $T_i=300 \text{ K}$ are given in Table 1.

Table 1 : *Nitrogen physical properties at $T_i=300 \text{ K}$*

k_i [W/m.K]	$C_{p,i}$ [J/kg.K]	ρ_i for $p_i=2 \text{ bars}$ [kg/m ³]	$\mu_i \cdot 10^5$ [Pa.s]	a_i [m/s]	r [J/kg.K]	$\gamma=C_p/C_v$	$\sigma_v=\sigma_T$
0,0259	1041	2,2466	1,782	353,07	296,8	1,4	1

Boundary conditions. The boundary conditions are:

$$\text{at } x=0, \forall y \in [0; H/2], p=p_i, \partial u/\partial x = 0, v=0 \text{ and } T=T_i \quad (5)$$

$$\text{at } x=L, \forall y \in [0; H/2], p=p_o, \partial u/\partial x = 0, v=0 \text{ and } \partial T/\partial x = 0 \quad (6)$$

$$\text{at } y=0, \forall x \in [0; L], \partial u/\partial y = 0, v=0 \text{ and } \partial T/\partial y = 0 \quad (7)$$

$$\text{at } y=H/2, \forall x \in [0; L], u|_s = \underbrace{\left(\frac{\sigma_v - 2}{\sigma_v} \right) \lambda \frac{\partial u}{\partial y}}_{1^{\text{st}} \text{ order velocity slip}} \Big|_s + \underbrace{\frac{3\mu r}{4p} \frac{\partial T}{\partial x}}_{\text{Thermal Creep}} \Big|_s, v=0 \text{ and } k \frac{\partial T}{\partial y} \Big|_s = q_w - \underbrace{\mu u_s \frac{\partial u}{\partial y}}_{\text{Visc. Stress Power}} \Big|_s \quad (8)$$

where $\lambda = \mu \sqrt{\pi r T} / \sqrt{2p}$ is the mean free path, r the nitrogen constant assimilated to an ideal gas and σ_v is the dynamic accommodation coefficient (see Table 1). As in [6], the wall is considered totally diffuse: $\sigma_v=1$. In Eq. (8), the subscript ‘‘s’’ means ‘‘slip’’ and refers to quantities evaluated in the gas close to the wall. The boundary condition (8) on u reflects the velocity slip and the thermal creep

(TC) at wall [1-3] and that on T reflects the conservation of the total heat flux density at wall [7-8]: $(-k\nabla T - \bar{\tau} \cdot \vec{v})_s = \vec{q}_w$, where $\vec{q}_w = q_w \cdot \vec{n}_w$ is the imposed heat flux density vector and \vec{n}_w is the unit vector at wall oriented towards the gas. In this relation, the viscous stress power (VSP) at the walls does not vanish due to the slip ($(\bar{\tau} \cdot \vec{v})_s \cdot \vec{n}_w \neq 0$). The solution of equations (1-8) provides the velocity and temperature fields of the gas, in particular the « slip » temperature, T_s , of the gas molecules close to the wall. When $0.01 < Kn < 0.1$, the wall temperature, T_w , is different of T_s due to the temperature jump at the wall. Then T_w is given by equation (9) where σ_T is the thermal accommodation coefficient ($\sigma_T=1$ for a totally diffuse wall).

$$T_w = T_s + \left(\frac{2 - \sigma_T}{\sigma_T} \right) \frac{2\gamma}{\gamma + 1} \frac{\lambda}{Pr} \left. \frac{\partial T}{\partial y} \right|_s \quad (9)$$

Numerical method. An in-house finite volume code is used to solve equations (1-8) discretized on a Cartesian grid. A second order centered scheme is used because the maximum Reynolds number is $Re_{max} < 25$ and the cell Reynolds number is $Re_{\Delta x} < 1$. The discrete nonlinear steady equations are solved in a coupled way by Newton's algorithm. The mesh size on each space direction is $N_x \times N_y = 9200 \times 30$. The mesh is uniform on x-direction and refined near the wall on y-direction, with a size ratio of two successive cells equal to 0.95. A sensitivity analysis to mesh refinement has shown that the solutions are well converged in all simulated cases. This code is very efficient to solve the present rarefied and compressible flows: starting from a previous case, only a few minutes are necessary to compute one case on a 2.4 GHz processor. It was then possible to carry out a parametric study of the influence of the inlet and outlet pressures requiring the computation of about 1000 different flow cases. The code has been validated through comparisons with experimental and numerical results [11, 12].

Analysis of the results

Definition of the variables analyzed. To characterize the flows, the maximum Knudsen number, Kn_o , the average Reynolds number, Re_o , and the maximum Mach number, Ma_o , at channel outlet are calculated, where $Kn = \lambda / (2H)$, $Re = 2 \dot{m} / \mu$, $Ma = u / (\gamma r T)^{1/2}$ and \dot{m} is the mass flow rate. To characterize the wall heat transfer, the mean Nusselt number is defined from q_w , T_w and the mean bulk temperature, T_b , by:

$$Nu_m = \frac{q_w HL}{\int_{x=0}^{x=L} k_s(x) (T_w(x) - T_b(x)) dx} \quad \text{with} \quad T_b(x) = \frac{2}{\dot{m}} \int_{y=0}^{y=H/2} \rho(x, y) u(x, y) T(x, y) dy \quad (10)$$

However the viscous stress power at the wall is frequently not taken into account in the thermal boundary condition (8) and, indirectly, in the definitions of T_w and Nu_m (Eqs. (9) and (10)). Thus, to characterize the influence of this term, the ratio between the average viscous stress power (VSP_m) and the imposed heat flux ($q_w L$) will be calculated as:

$$\frac{VSP_m}{q_w L} = \left[\int_{x=0}^L \mu_s u_s \left. \frac{\partial u}{\partial y} \right|_s dx \right] / q_w L \quad (11)$$

Likewise, many studies have neglected the influence of the pressure work (PW) and/or viscous dissipation (VD) in the energy equation (3). Sun and Jaluria [6] showed that the wall heat transfer is directly correlated to the sum $PW+VD$ and to the ratio PW/VD . We will therefore consider the ratio between these two terms defined as follows, with Ω the volume of the computational domain:

$$\frac{PW_m}{VD_m} = \left[\iint_{\Omega} \vec{v} \cdot \nabla p \, d\Omega \right] / \left[\iint_{\Omega} \bar{\tau} : \nabla \vec{v} \, d\Omega \right] \quad (12)$$

Parametric study of the inlet and outlet pressure influence. A parametric study of the influence of the inlet and outlet pressures on the nitrogen flows and the associated heat transfer has been conducted. Flows for about 1000 couples (p_i, p_o) have been calculated to cover the pressure ranges $0.9 < p_i < 5$ bars and $0.08 < p_o < 4.9$ bars. The maximum bulk temperature, $T_{b,max}$, close to the outlet of the channel, the mass flow rate, \dot{m} , and all the quantities defined in the above subsection have been calculated for each simulated flow. The maps of the isovalues of these quantities are plotted in Fig. 2 vs. $\Delta p/p_o$ and p_o , where $\Delta p = p_i - p_o$.

The maximum pressures of the study domain are limited to 5 bars to satisfy the assumption of ideal gas. Furthermore the physical model used (Eqs. (1-8)) is not valid for the whole pressure range scanned. Then we first identify the pressure ranges for which $Kn_o < 0.1$ (validity of the continuous model with slip), $Ma_o < 1$ (no shock wave), $Re_o < 2000$ (validity of the laminar model) and $T_{b,max} < 2000$ K (rough limit of the thermal resistance of the materials used). The graphs (a, d, f, g) of Fig. 2 show the isovalues of these parameters and the resulting limits. The limit related to the validity of the laminar model does not act ($Re < 25$ everywhere) and $Ma_o < 1$ almost everywhere when $p_i < 5$ bar.

Isocontours of the ratio TC/u_s of the thermal creep term to the slip velocity (Eq. (8)) are plotted in Fig. 2(c). Here we consider that the thermal creep begins to have an influence on u_s when the maximum of TC/u_s on the channel wall is greater than 10%. The limit $\max(TC/u_s) = 0.1$ is plotted on the graphs of Fig. 2 (black bold line). Figure 2(d) shows that it corresponds to $Re_o < 0.2$ to 0.5. In other words, thermal creep only occurs at very small Re values. It is therefore necessary to take into account the momentum and heat diffusion, in upstream and downstream sections of the channel, for realistic simulations of the thermal creep. For example, extensions at the inlet and at the outlet of the channel should be introduced to properly model this phenomenon.

There are three groups of graphs having globally the same shape of the isocontours in Fig. 2: these groups are (a, b), (c, d, e, f) and (g, h, i). Therefore each group gathers up quantities that are correlated between themselves. As already analyzed in [6], the group of graphs (a, b) confirms that the amplitude of the ratio PW_m/VD_m of the pressure work to the viscous dissipation is correlated to the rarefaction rate, here defined by the outlet Knudsen number, Kn_o . For no slip flows and when Knudsen number is small ($Kn_o < 0.01$), Figs. 2(a, b) indicate that $PW_m/VD_m \approx -1$: it is indeed well known that $PW(<0)$ and $VD(>0)$ compensate each other for no slip flows. This is no longer valid for slip flows: here PW_m/VD_m can reach -2 when $Kn_o = 0.1$ which means that pressure work (heat sink) dominates viscous dissipation (heat source). As a consequence, PW and VD cannot be neglected for large values of Kn_o (see next subsection).

In Fig. 2, the group of graphs (c, d, e, f) shows that the maximum bulk temperature reached near the outlet, $T_{b,max}$, the influence of the thermal creep on the slip velocity, TC/u_s , and the mass flow rate, \dot{m} , are directly correlated to the Reynolds number, Re_o . TC/u_s and $T_{b,max}$ are maximum at low flow rate. The group of graphs (g, h, i) indicates that the average Nusselt number, Nu_m , and the ratio $VSP_m/q_w L$ of the viscous stress power at the walls to the imposed heat flux are correlated with the Mach number, Ma_o , only for $Re_o > 1$. For $Re_o < 1$, Nu_m is correlated with Kn_o (see Fig. 2(a)). We don't know if this behavior is due to the influence of the rarefaction or if this is a numerical artifact due to the upstream diffusion and the inlet thermal boundary condition used ($T = T_i = 300$ K).

For $Re_o > 1$, Nu_m decreases when $VSP_m/q_w L$ increases. Indeed, the imposed heat flux, q_w , is constant and the viscous stress power $VSP_m > 0$ (Eq. (8)). Thus, when the magnitude of VSP_m increases, $(\partial T/\partial y)_s$ and the temperature jump at the wall (Eq. (9)) increases. Therefore, in Eq. (10), $T_w - T_b$ increases since $T_s \approx T_b$ and Nu_m decreases. In the present case, we have checked (not shown here) that the term VSP_m (Eq. (11)) is equal to 40% to 90% of the integral of the conduction flux transmitted to the fluid, $\int_{x=0}^L k[\partial T/\partial y]_s dx$, over the half of the studied parameter domain (for $VSP_m/q_w L > 0.2$ in Fig. 2(h)): therefore VSP_m cannot be neglected in the heat flux balance.

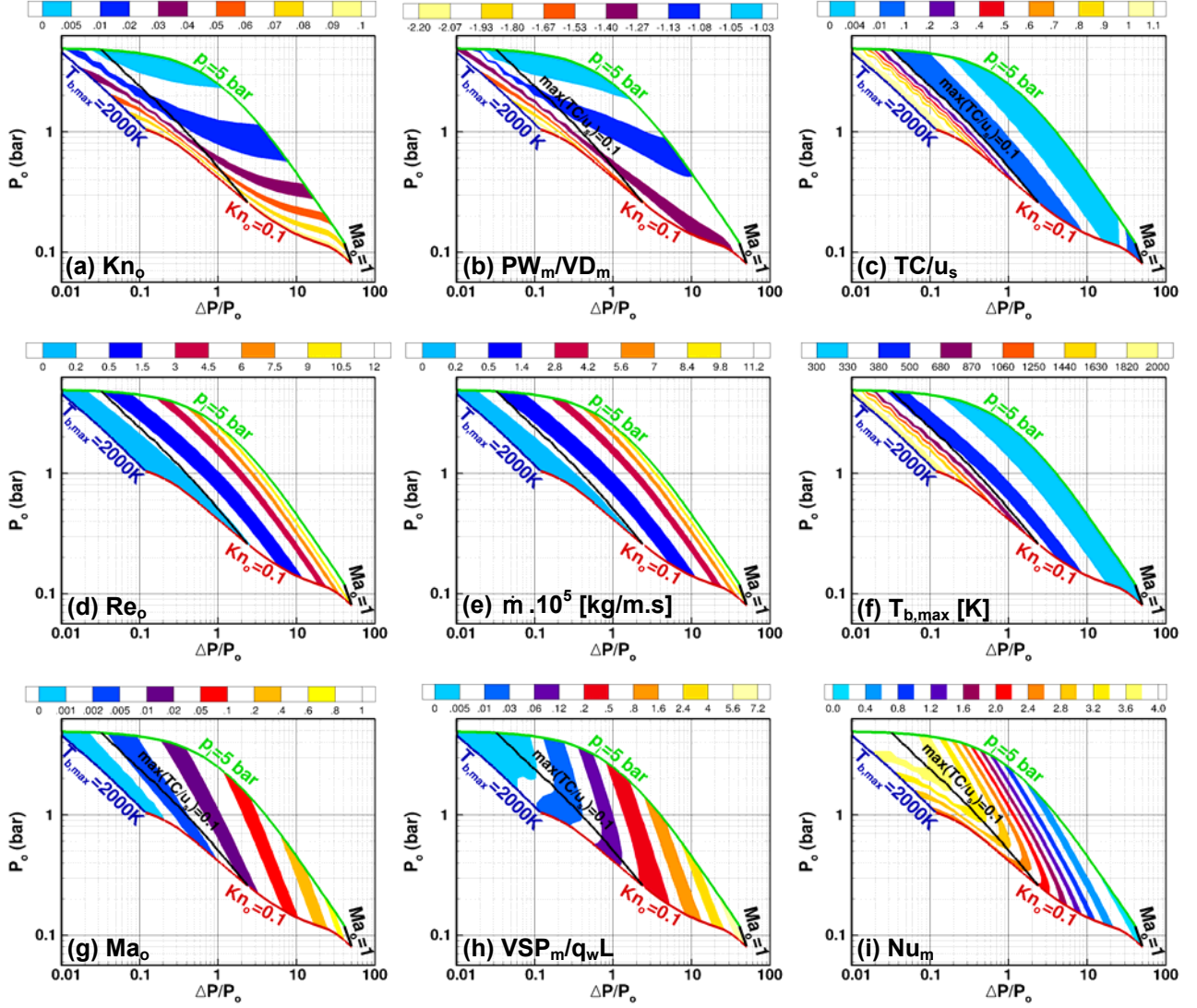


Figure 2 : Isocontours of the different quantities analyzed (noted on the bottom left of each graph) in the plane $\Delta p/p_o$ (abscissa) - p_o (ordinate) and validity limits of the used model.

Comparison of complete and simplified models. Simplified models that do not consider the thermal creep (TC) and/or the viscous stress power (VSP) at the wall and/or the pressure work (PW) and the viscous dissipation (VD) are often used in the literature. In Fig.3, we analyze the influence of such models on the mass flow rate, the maximum bulk temperature and the mean Nusselt number. Figure 3 presents isocontours of the relative errors on these quantities defined by: $\%er(f) = (f_c - f_s)/f_c \times 100$, where $f = \dot{m}$, $T_{b,max}$ or Nu_m and f_c is the solution of the complete present model (Eqs. (1-8)) and f_s is the solution of a simplified model as mentioned on each graph of Fig.3.

As already seen above and confirmed by Figs. 3(a, b), it is possible to ignore the thermal creep on a very large domain of pressures. Indeed, the relative errors between the simplified and complete models on $T_{b,max}$ and \dot{m} are greater than 5% and reach 40% at maximum only for $Re_o < 0.2$ (see Fig. 2(d)). In the same zone, the maximum relative error on Nu_m is 20% (not shown here). Likewise, Fig. 3(c) confirms that PW and VD cannot be neglected for large values of Kn_o (> 0.03) and small outlet pressures ($p_o < 0.4$ bar) since the relative errors on $T_{b,max}$ varies between 10 and 25% in this case. But, to ignore PW and VD mainly generates errors on the heat transfer since relative errors of 400% can be measured on Nu_m for large inlet pressures and large pressure differences Δp (see Fig. 3(d)). Finally, to neglect the viscous stress power, VSP, at the walls in the model can generate relative errors of 12% on $T_{b,max}$ and 80% on Nu_m (Figs. 3(e, f)). These errors are present in the zone where the contribution of the viscous stress power to the total heat flux imposed at the wall is maximum (see Fig. 2(h)) and the Knudsen number is large ($Kn_o > 0.03$ in Fig. 2(a)).

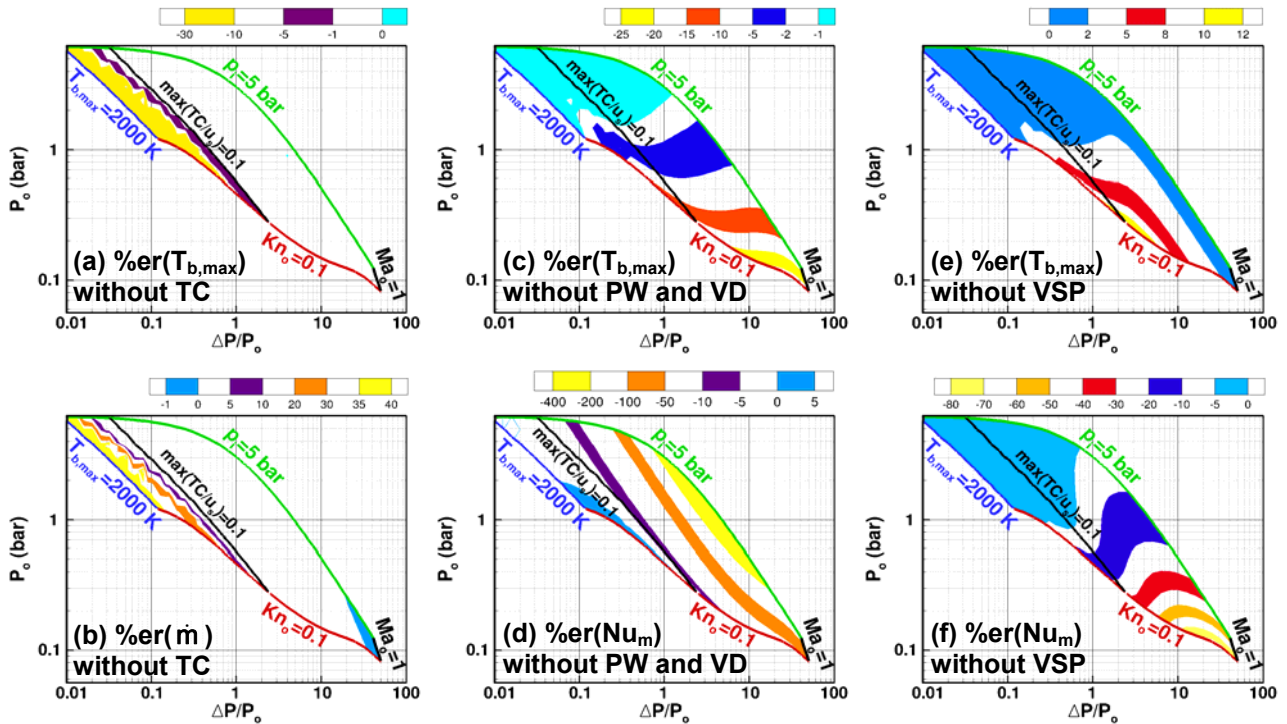


Figure 3 : Relative errors, %er, on \dot{m} , $T_{b,max}$ or Nu_m for simplified models without thermal creep (TC) or viscous stress power at wall (VSP) or pressure work and viscous dissipation (PW and VD).

Conclusion

The present numerical simulations have shown that the viscous stress power at the wall, the pressure work and the viscous dissipation can not be neglected on a large part of the parameter domain corresponding to laminar compressible flows of perfect gas in micro-channels. It has also been shown that the thermal creep can be influential only at very small Reynolds and Péclet numbers; therefore the simulation of such a phenomenon requires, to be realistic, to take account of the momentum and heat diffusion upstream and downstream of the channel. Finally, correlations between the different quantities and the dimensionless parameters Kn, Re, Ma characterizing this type of flow and the associated heat transfer have been determined graphically.

References

- [1] S. Colin: Microfluid Nanofluid, Vol. 1 (2005), p. 268-279.
- [2] S. Colin: J. Heat Transfer, Vol. 134 (2012), 020908.
- [3] G. Karniadakis, A. Beskok, N. Aluru: *Microflows and nanoflows: Fundamentals and simulation* (Springer, New York 2005).
- [4] H. P. Kavehpour, M. Faghri, Y. Asako: Numerical Heat Transf. A, Vol. 32 (1997), p. 677-696.
- [5] C. Hong, Y. Asako, J.-H. Lee: Int. J. Thermal Sciences, Vol. 46 (2007), p. 1153-1162.
- [6] Z. Sun, Y. Jaluria: Int. J. Heat Mass Transfer, Vol. 55 (2012), p. 3488-3497.
- [7] E. M. Sparrow, S. H. Lin: J. Heat Transfer, Vol. 84 (1962), p. 363-369.
- [8] C. Hong, Y. Asako: Int. J. Heat Mass Transfer, Vol. 53 (2010), p. 3075-3079.
- [9] A. Qazi Zade, M. Renksizbulut, J. Friedman: Int. J. Heat Fluid Flow, Vol. 32 (2011), p. 117-127.
- [10] Z. Sun, Y. Jaluria: J. Elect. Packaging, Vol. 133 (2011), 021008.
- [11] C. Tchekiken, E. Chénier, X. Nicolas, G. Lauriat, *A propos de la modélisation numérique de la convection de gaz en micro conduites*, Congrès Français de Thermique, Lyon, France (2014).
- [12] C. Tchekiken, X. Nicolas, L.-H. Baudey-Laubier, G. Lauriat, *Simulation numérique d'écoulements anisothermes de gaz en micro canal : effets de compressibilité et de glissement*, 21^{ème} Congrès Français de Mécanique, Bordeaux, France (2013).